Available online at www.sciencedirect.com
SCIENCE DIRECT®
Organic Geochemistry 35 (2004) 355–375
Organic Geochemistry
www.elsevier.com/locate/orggeochem

Mineral mesopore effects on nitrogenous organic matter adsorption

Andrew R. Zimmerman[a,*], Keith W. Goyne[b], Jon Chorover[b], Sridhar Komarneni[c], Susan L. Brantley[a]

[a]Department of Geosciences, The Pennsylvania State University, University Park, PA 16802, USA
[b]Department of Soil, Water and Environmental Science, University of Arizona, Tucson, AZ 85721, USA
[c]Department of Crop and Soil Sciences, Materials Research Institute, The Pennsylvania State University, University Park, PA 16802, USA

Received 15 April 2003; accepted 14 October 2003
(returned to author for revision 22 July 2003)

Abstract

The "mesopore protection hypothesis" [Chem. Geol. 114 (1994) 347; Geochim. Cosmochim. Acta 58 (1994) 1271] proposes that organic matter (OM) may be protected from enzymatic degradation by sequestration within mineral mesopores (2–50 nm diameter). This hypothesis is a leading, though controversial, theory in explaining both the preservation of some extremely labile OM compounds and observed correlations between OM content and mineral surface area in soils and sediments. To test this idea, we carried out batch experiments in aqueous suspensions to examine the adsorption/desorption of amino acid monomers and polymers onto fabricated mesoporous and nonporous alumina and silica. Each mineral pair was of similar surface chemistry and differed only in the presence or absence of intraparticle mesoporosity. All amino acid monomers and polymers smaller than about one-half the pore diameter exhibited significantly greater surface area-normalized adsorption to mesoporous alumina (8.2 nm mean pore diameter) and silica (3.4 nm mean pore diameter) compared to nonporous mineral analogues. Proteins larger than the mesopores exhibited greater adsorption to the nonporous phases indicating their exclusion from internal surfaces of mesoporous minerals. Greater desorption hysteresis for mesopore-sorbed OM indicates that desorption from pores was inhibited. The adsorption/desorption data, as well as Langmuir-Freundlich modeling and adsorption affinity distributions, suggest that capillary condensation, a 'pore-filling' mechanism, may explain the experimental observations. These results provide a potential mechanism for the selective sequestration and preservation of sedimentary OM as well as organic contaminants.

1. Introduction

Organic matter (OM)–mineral interactions are of central importance in explaining such diverse phenomena as sequestration of pollutants in soils and sediments (Luthy et al., 1997), turnover of natural soil organic carbon (Torn et al., 1997), and preservation of organic carbon in coastal and marine sediments (Mayer, 1994b, 1999). Upon release from biota (i.e., plants, algae and microbes), biomolecules may be sequestered within soils and sediments or may remain entrained in solution, depending on their affinity for the solid and aqueous phases. Near-surface carbon sinks are transient in nature, and much of this biomolecular OM is degraded by microorganisms to humic substances and CO_2 (Zibilske, 1994; Moore, 1997). Although most biomolecular OM is inherently labile, some portion of it is preserved in

* Corresponding author.
E-mail address: azimmer@geosc.psu.edu (A.R. Zimmerman).

0146-6380/$ - see front matter © 2003 Elsevier Ltd. All rights reserved.
doi:10.1016/j.orggeochem.2003.10.009

soils and sediments and remains apparently unavailable to microbial decomposition processes (Hedges and Keil, 1995; Luthy et al., 1997). The factors that govern the amount and nature of OM sequestered in this manner are of fundamental importance to our understanding of the migration, bioavailability and remediation of organic contaminants, global carbon cycling and the availability of organic soil nutrients to plants.

Direct correlations between soil and sediment surface area and organic carbon are commonly observed (e.g., Mayer et al., 1988; Keil, 1994; Bergamaschi et al., 1997; Baldock and Skjemstad, 2000; Zimmerman and Canuel, 2001; Kennedy et al., 2002) suggesting that OM-mineral complexation can stabilize labile forms of OM against microbial attack (Jastrow and Miller, 1997; Kaiser and Guggenberger, 2000). Because mineral surfaces are often dominated by the internal surfaces of mesopores (2–50 nm in diameter; Mayer, 1994a), some workers have suggested that mineral mesopores may play a major role in the sequestration and preservation of OM in sediments by protecting OM from degradative attack by bacteria or bacterial extracellular enzymes by physical occlusion within mineral pores (Mayer, 1994a,b; Harms and Bosma, 1996; Hulthe et al., 1998). Additional experiments have indicated that $<15\%$ of the total aluminosilicate surfaces are coated with OM, suggesting that OM is present in localized patches (Ransom et al., 1997; Mayer, 1999) such as within pores.

Additional lines of evidence supporting the 'mesopore protection hypothesis' are found in thermodynamic and kinetic studies of organic contaminant adsorption and desorption. Cycling of organic carbon in sediments and soils has been generally characterized by complex kinetics in which fast and slow processes of carbon degradation are observed (Luthy et al., 1997). Fast cycling has been related to biodegradation of readily available OM whereas slow cycling has been attributed to the occurrence of a less available portion of the OM. This latter more recalcitrant OM may be inherently recalcitrant or it may be associated with pores in geological materials.

Several possible physical and chemical mechanisms for the sequestration of OM within mesopores have been suggested based upon extrapolation from studies of hydrophobic organic contaminants (HOCs) that indicate enhanced organic compound retention in mineral micropores. Molecules sorbed in mineral micropores are subjected to stronger adsorption energies due to compound interaction with pore walls (Farrell and Reinhard, 1994). Steric effects may also inhibit organic compound removal from such pores (Luthy et al., 1997). Restricted transport has been shown to impede compound desorption in micropores due to slow diffusion and high tortuosity (Farrell and Reinhard, 1994; Luthy et al., 1997). Lastly, the concentration of reactants within micropores may favor condensation-type reactions and, therefore, may play a role in OM sequestration as well as kerogen formation (Collins et al., 1995). Although these retention mechanisms have been associated with HOCs in micropores, it is reasonable to propose that similar processes could govern hydrophilic and macromolecular OM sequestration in mineral mesopores.

The goal of this study was to test the feasibility of the 'mesopore protection hypothesis' by examining the effect of mesoporosity on the adsorption/desorption of amino acids and proteins. For 'mesopore protection' to be a viable OM preservation mechanism, we posit that (1) small organic compounds must be able to sorb to the internal surfaces of mineral mesopores, (2) bond energies on internal surfaces must be strong enough to inhibit desorption, and (3) larger compounds (e.g., proteins, enzymes) must be inhibited from entering pores. If these processes occur, we predict that mesopores on a mineral surface will enhance adsorption and inhibit desorption of small organic molecules relative to nonporous mineral surfaces. Furthermore, we expect to see more adsorption/desorption hysteresis (non-equivalence of sorption and desorption isotherms) for mesoporous versus analogous nonporous material. We also predict that, above a threshold size, larger molecules will exhibit less adsorption to mesoporous versus nonporous mineral surfaces. Therefore, additional goals of this research were to determine the size range of representative organic compounds that may sorb to internal surfaces of the mesopores as well as the associated sorption mechanism(s).

To test these predictions, we conducted a series of batch equilibrium adsorption/desorption experiments by reacting amino acid monomers, dimers, trimers and polymers (proteins) of varying size, charge and functionality with fabricated mineral analogues (silica and alumina) containing controlled and uniform mesoporosity. Amino acids were used as model organic compounds because of their ubiquity in the environment and because they are often found in severely degraded soils and sediments even though they are readily biodegradable (e.g., Boyd and Mortland, 1996; Zang et al., 1997). Recent research has shown that proteinaceous material can survive diagenesis with very little alteration (Zang et al., 1997, 2001; Riboulleau et al., 2002). Additionally, the amine and carboxyl moieties of amino acids are predominant in a wide variety of natural OM such as lignins and humic materials.

Silicon and aluminum oxides were chosen as sorbents because they represent surfaces that are prevalent in natural environments and they exhibit very different surface chemical properties, thus providing a strong contrast in reactivity. For example, the point of zero net charge (p.z.n.c.) of SiO_2 is pH 2.0, whereas that of Al_2O_3 is pH 8.7 (Sposito, 1984). Thus, silica is primarily negatively charged throughout the pH range of natural

waters, whereas alumina is positively charged except under highly alkaline conditions. The hydroxylated surfaces of weakly acidic Fe and Al oxides and hydroxides have been shown to promote strong binding of carboxylated, aromatic OM through a ligand exchange mechanism (Gu et al., 1994, 1995; Ochs et al., 1994; Chorover and Amistadi, 2001). In contrast, OM sorption to silicates has been attributed to physical forces such as hydrophobic and entropy effects (Jardine et al., 1989; Baham and Sposito, 1994; Chorover and Amistadi, 2001).

While the high density of uniform size and shape mesopores that characterizes the synthetic materials used is unlikely to be found in natural sediment or soil mineral surfaces, they serve as model surfaces to investigate the processes of OM adsorption into pores. Intraparticle mesopores are abundant in natural materials, however, and have been found to be sites of a significant portion, even a majority, of surface area in many depositional systems including soils (Pennell et al., 1995), aquifer sands (Werth and Reinhard, 1997; Ball et al., 1990), and marine and estuarine sediments (Mayer, 1994b, 1999). Mesoporosity, in the form of altered and aggregated clay, may be either intra- or interparticle and has also been found to control surface area in some sediment (Bock and Mayer, 2000; Neaman et al., 2003; Temuujin et al., 2003). Other geomaterials that have been found to contain significant mesoporosity include suspended particles in estuaries (Titley et al., 1987), weathered and laboratory-ground primary minerals (Zhang et al., 1993; Anbeek et al., 1994; Hodson, 1998; Brantley et al., 1999; Brantley and Mellot, 2000), and diatom tests (Vrieling et al., 1999). Finally, OM reactions with natural materials containing small mesopores or large micropores, including zeolites (Li and Werth, 2001), organic matter such as soot (Rockne et al., 2000), humic material and kerogen (de Jonge and Mittelmeijer-Hazeleger, 1996; Malekani et al., 1997; Huang et al., 2003), and intercalated clay minerals (Theng, 1974; Kostoglod et al., 1998) may play a role in OM preservation in some systems.

2. Experimental

2.1. Mineral sorbents

Mesoporous mineral analogues were fabricated to contain known pore sizes of unimodal distributions. These phases, also known as mesoporous molecular sieves (such as MCM-41), are expected to find applications as molecular sieves and catalysts in the petroleum industry. The amorphous mesoporous alumina (Al_2O_3) and silica (SiO_2) minerals used here were synthesized by the neutral template route (Komarneni et al., 1996). Briefly, dodecylamine was stirred in water and ethanol and then aluminum isopropoxide or tetraethyl orthosilicate was added. The material was then heated (540°, 6 h) to remove the organic template leaving only the inorganic support. Nonporous silica and alumina (γ-Al_2O_3) were purchased from Alfa Aesar (Ward Hill, MA; stock Nos. 40007 and 89709, respectively). These materials were chosen for the similarity of their surface chemistry to that of their mesoporous analogues. The nonporous alumina was washed prior to use (0.2 kg l^{-1} in 0.02 M $CaCl_2$, 24 h, 5×). All the above minerals were analyzed by elemental analyzer and found to contain undetectable (<0.2 wt.%) organic carbon contamination. A detailed description of the surface chemistry and morphology, including a plot of pore-size distribution of these materials has been published elsewhere (Goyne et al., 2002), but is summarized here (Table 1). Specific surface area and pore structure of the minerals were determined by N_2 sorptometry (ASAP 2010, Micromeritics).

Table 1
Mineral surface characteristics

Mineral phase	Specific surface area[a] (m^2 g^{-1})	Mean pore diameter[b] (nm)	Total pore volume[b] (cm^3 g^{-1})	Framework pore surface area (%)[b,c]	Positive charge density at pH 5.7 (nm^{-2})[d]	Net charge density at pH 5.7 (nm^{-2})[d]	p.z.n.c.[d]
Mesoporous alumina	242 (±5.9)	8.2 (±0.6)	0.6 (±0.03)	96.5	+ 0.60	+ 0.45	6.47
Nonporous γ-alumina	37 (±3.3)	20 (±3)	0.20 (±0.01)	–[e]	+ 0.69	+ 0.52	6.66
Mesoporous silica	700 (±11.9)	3.43 (±0.02)	0.91 (±0.01)	99.7	0	−0.15	<2.85
Nonporous silica	7.5 (±0.1)	14 (±2)	0.024 (±0.003)	–[e]	0	−0.28	<2.82

[a] Determined by multi-point N_2 adsorption and Brunauer-Emmett-Teller (BET) calculation method (mean±S.D.).
[b] Determined by N_2 sorptometry and BJH calculation method (Barrett et al., 1951) on the adsorption branch (mean±S.D.).
[c] Framework, or intraparticle porosity, is defined as pores smaller than 20 and greater than 2 nm diameter. This was done because we estimate that interparticle pores >20 nm are likely given the small particle size (about 0.1 μm) of the nonporous minerals.
[d] Determined by ion and proton adsorption techniques via discontinuous titration (Goyne et al., 2002).
[e] No framework porosity.

Surface area was calculated using multi-point adsorption data from the linear segment of the N_2 adsorption isotherms using Brunauer-Emmett-Teller (BET; Brunauer et al., 1938) theory. Pore size distributions were calculated from adsorption branch isotherms using the Barrett-Joyner-Halenda (BJH) method (Barrett et al., 1951), assuming the pores to be cylindrical, perpendicular to the mineral surface and closed on one end, and using the Halsey layer thickness equation (Halsey, 1948).

Transmission electronic microscopy was carried out to confirm the lack of intraparticle pores in the 'non-porous' minerals. The results of proton titration and ion adsorption experiments indicate that the surface charge density of both alumina and silica pairs were similar at the experimental pH and differed only in surface morphology (Goyne et al., 2002).

2.2. Adsorption experiments

For each organic compound, batch adsorption/desorption (5 day/5 day) experiments were carried out in duplicate on each mineral analogue. The five day adsorption/desorption period was chosen based upon preliminary experiments that determined the great majority of adsorption to occur within about 2 days. The polypropylene centrifuge tubes (50 ml) used to contain the mineral and aqueous solution did not significantly sorb any of the compounds examined. Sorption experiments were conducted using the equivalent of 80 m^2 surface area for each mineral (50–1330 mg) in 25 ml aqueous background solution approximating natural sediment/soil conditions (0.02 M $CaCl_2$ and pH 5.7). $HgCl_2$ (200 mg l^{-1}) was added to prevent bacterial growth and did not significantly influence adsorption of amino acids. Rather than use a buffer that might compete for adsorption sites, pH was maintained by the addition of a predetermined amount of HCl for the alumina minerals or $Ca(OH)_2$ for silica minerals. The tubes were placed on end-over-end spinners in the dark (10 rpm, 22 °C) for the adsorption period. After the reaction, tubes were centrifuged (1 h, 4500 rpm) and the supernatant was removed, analyzed and replaced with 25 ml organic-free background solution prior to the desorption period. Adsorption isotherms were constructed for each amino acid compound by measuring adsorption over concentrations ranging from the minimum detectable to the maximum dissolvable concentration.

Amino acid concentrations were measured on a fluorometer (Fluoro-Tec, St. John Assoc., Inc.; excitation: 320 nm, emission: 450 nm) after derivatization with a fluorescent tag, *ortho*-phthaldialdehyde, using the method of Lindroth and Mopper (1979) with modification (Confer et al., 1995). This method was used for the analysis of amino acid monomer, dimer and polymer concentrations by diluting solutions with the background electrolyte solution to give concentrations within the predetermined range of linear fluorescent response. The amount of a compound adsorbed (μmol m^{-2}) was calculated as the difference between the amino acid concentration in solution in tubes containing the mineral and a control tube with the compound solution and no mineral. Compound desorption was calculated as the difference between the initial amount in solution (calculated by weighing tubes after decanting the overlying solution and assuming a density of 1 g ml^{-1} for the entrained solution) and the final amount in solution after 5 days and centrifugation (1 h, 4500 rpm).

The amino acid monomers and polymers used as sorbates ranged in molecular weight from 57 to 169,000 Daltons (Table 2). They were purchased from Sigma (racemized forms where applicable) and used without further purification. Molecular sizes of these molecules were estimated in two ways. For monomers, dimers and

Table 2
Amino acid compound characteristics

Compound	Net charge at pH 5.7	Molecular weight (Dalton)	Estimated molecular diameter (nm)[a]
Glycine	0	57	0.6 × 0.35
Lysine	+1	128	0.8 × 0.35
Glutamate	−1	129	0.8 × 0.35
Tryptophan[b]	0	186	0.8 × 0.35
Diglutamate	−2	276	1.2 × 0.5
Ditryptophan[b]	0	390	1.4 × 0.5
Triaspartate	−4	363	1.2 × 0.6
Lysozyme[b]	+8	14,300	4 × 3
Albumin[b]	−18	66,000	15 × 4
γ-Globulin[b]	+1	169,000	24 × 4

[a] Estimate of major and minor molecular dimension as described in text.
[b] Contains hydrophoboic moiety.

trimers, nominal dimensions were determined by measuring interatomic distances and accounting for van der Waal's radii of the atoms on molecular structures determined with energy minimization using the COMPASS force field (Sun, 1998). No conformational changes such as those that might take place in solution were considered. The proteins chosen for these experiments are all globular proteins and are thought to behave as 'hard' particles (Arai and Norde, 1990). Molecular size estimates of the protein were made by assimilating a diverse array of data from web and print sources including polyacrylamide disc electrophoresis, gel electrophoresis, capillary electrophoresis, gel filtration chromatography, light and X-ray scattering and hydrodynamic experiments.

2.3. Isotherm models

Adsorption isotherms were modeled using the Langmuir-Freundlich (LF) isotherm, also known as the Sips equation (Sips, 1948). This model describes an equilibrium relationship between the concentration of a sorbed compound (S) and the equilibrium compound concentration in solution (C) such that:

$$S = \frac{NbC^m}{1 + bC^m} \tag{1}$$

where N, b, and m are three fitting coefficients that represent the adsorption capacity, the binding affinity of the compound, and the heterogeneity of site energies, respectively. As b approaches zero at low binding affinities, the equation reduces to the classical Freundlich equation. As m approaches unity, indicative of a completely homogeneous sorbent surface (i.e. energetic equivalence of all binding sites) the equation reduces to the classical Langmuir equation (Langmuir, 1916). Thus, the hybridized LF isotherm is able to model adsorption of solutes at high and low concentrations onto homogeneous and heterogeneous sorbents. The LF isotherm was fit to the experimental data following the method of Umpleby et al. (2001) in which the solver function of Microsoft Excel 2002 is used to maximize the coefficient of determination (R^2) by iteratively varying the three fitting parameters N, b, and m. R^2 is calculated from the sum of residuals, i.e. the difference between the experiment and model-predicted sorbed concentrations.

Adsorption/desorption hysteresis is often indicative of pore-filling, capillary condensation or unique sorbate-sorbent interaction within pores. To quantify the degree of hysteresis, we have modified the method of Huang and Weber (1997) and Huang et al. (1998) in which a desorption hysteresis index (HI) is calculated as:

$$HI = \frac{S_i^d - S_{i(LF)}^a}{S_{i(LF)}^a} \tag{2}$$

where S_i^d refers to the sorbed concentration measured after the desorption step and $S_{i(LF)}^a$ refers to the sorbed concentration calculated by the LF isotherm fitted to the adsorption data [Eq. (1)], both for solution concentration i. While Huang and Weber (1997) and Huang et al. (1998) specify a few solution concentrations with which to make comparisons, we calculate an HI for all the desorption data points collected for each compound and use the mean, HI_{mn}, for comparison purposes.

Thermodynamic binding properties of a sorbate can be extracted directly from fitting parameters of isotherm models such as the Langmuir model that assume a homogeneous sorbent. Energetically heterogeneous surfaces, however, must be characterized by an affinity distribution function. Expression of a continuous distribution of binding site energies takes the form of a Fredholm integral that has no analytical solution (Geng and Loh, 2001). However, numerous approximation methods have been developed. We follow the approach of Umpleby et al. (2001) who developed an equation that gives the number of binding sites (N_i) for a given association constant (K_i) using the fitting parameters of the LF model. This model has been shown to yield results similar to other approximation methods but is better behaved in a variety of circumstances (Umpleby et al., 2001).

2.4. Spectroscopy

Diffuse reflectance infrared Fourier transform (DRIFT) spectroscopy was used to obtain information on sorbate-sorbent bond type and strength. After batch adsorption experiments, minerals with sorbed amino acids (maximum adsorption obtainable) were centrifuged, supernatant removed, and immediately frozen (−80 °C). Within a few days, samples were freeze-dried, ground and mixed with ground KBr powder (Spectra-Tech, Inc.) to give a powdered sample concentration of 100 g kg^{-1}. Other samples were placed on a silicon carbide disk and analyzed undiluted. All DRIFT spectra were obtained by averaging 400 scans at 2 cm^{-1} resolution on a Nicolet Magna 560 spectrometer. Mineral analogues with no sorbed amino acid were also analyzed for comparison.

3. Results

3.1. Compound sorption—general observations

Of the amino acid monomers and polymer compounds tested (those listed in Table 2 as well as dilysine,

tetra-aspartic acid and insulin, data not shown), all except net positively charged lysine and dilysine displayed measurable sorption to both mesoporous alumina (MP-Al) and nonporous alumina (NP-Al) minerals. Of the monomers and oligomers tested, only tryptophan and ditryptophan sorbed to either mesoporous silica (MP-Si) or nonporous silica (NP-Si). Most surprisingly, positively charged lysine (+1) and dilysine (+2) did not measurably adsorb to the negatively charged silica surface though these compounds strongly sorb to clay minerals and sediments (Hedges and Hare, 1987; Henrichs and Sugai, 1993; Wang and Lee, 1993). In addition, all the proteins, even those with large net negative charges, sorbed to silica. Quantitative intermolecular trends and comparisons between minerals can only be made by comparing sorption at equivalent equilibrium concentrations using a modeling approach (in discussion section).

3.2. Adsorption-desorption isotherms

The adsorption isotherms are plotted, by convention, on a log-log scale. Here, sorbed concentrations are normalized to surface area so that direct comparisons between porous and nonporous phases may be made. Adsorption measurements made in duplicate were, in all cases except those of very low concentration, in close agreement. Larger variations were observed for duplicate desorption measurements due, presumably, to the larger analytical error associated with removing the supernatant and estimating the remaining entrained solution.

The adsorption isotherms for most amino acids and proteins on alumina (Fig. 1) and silica (Fig. 2) are nonlinear and generally concave downward on both a normal and log–log scale. These isotherms may be classified as type IV (Brunauer, 1943) and exhibit, in most cases, evidence of high surface affinity and surface saturating behavior. Isotherms of this shape are commonly observed for the adsorption of ionic organic compounds to minerals (Schwarzenbach et al., 1993). With the exception of glycine, ditryptophan, and lysozyme on alumina, and tryptophan on silica, adsorption maxima plateaus were reached at high solution concentrations.

For glycine and glutamate on alumina, and for tryptophan on silica, desorption isotherms followed adsorption isotherms, within analytical error. That is, they were non-hysteretic and indicative of complete adsorption reversibility. All other compounds exhibited varying degrees of desorption hysteresis. For diglutamate on MP-Al, there was no measurable desorption i.e. adsorption was completely irreversible. In this case and others where desorption was undetectable, an equilibrium solution concentration of 3.2×10^{-4} μM (minimum detectable) was assigned for the purposes of graphing and modeling. Quantitative evaluation of the extent of desorption hysteresis are presented in the following discussion.

3.3. Ancillary data

Measurements of mineral surface area and pore volume before and after adsorption/desorption experiments provide evidence for compound adsorption and retention on the internal surfaces of mesopores. Control samples with no sorbed compounds recorded slight decreases in surface area and increases in pore volume (about 10%) due to mineral dissolution. Relative to control minerals, the surface area of MP-Al decreased by 2.4% after the sorption of glycine (Table 3). Although this change was not greatly different from that of NP-Al, the pore volume decrease of MP-Al with sorbed glycine was much greater (5 versus 1%). Similarly, only pore volume, and not surface area, decreased (6.7%) after the sorption of tryptophan to MP-Al. Both surface area and pore volume decreases for MP-Al were more dramatic, however, following the sorption of glutamate (14.1 and 16.5%, respectively) and ditryptophan (21.9 and 22.8%, respectively) versus much smaller changes after the sorption of these compounds to NP-Al. Even greater decreases in surface area and pore volume were observed after the sorption of albumin and γ-globulin to MP-Al and MP-Si, presumably because pore openings were blocked by these larger proteins.

Loadings of only a few compounds, glutamate, diglutamate, tryptophan and dihydroxyphenylalanine, were great enough to obtain infrared (DRIFT) absorption signals of sufficient intensity for analysis. We observed differences between the porous-sorbed versus nonporous-sorbed spectra of only glutamate (Fig. 3) and diglutamate (not shown). We attribute the absorption bands in the 3500, 1600 and the 1400 cm^{-1} region, to sorbed water (OH–H) and amine (N–H), asymmetric carboxylate (COO^-), and symmetric carboxylate bond stretching, respectively (Gu et al., 1995; Vermohlen et al., 2000). The adsorption band of glutamate and diglutamate sorbed to NP-Al at 1615 cm^{-1} was shifted downward by 45 and 27 cm^{-1}, respectively, when these compounds were sorbed to MP-Al. This decrease in bond frequency may be indicative of a stronger bond environment for mesoporous versus nonporous-bound amino acids, and shall be discussed further in the following section.

4. Discussion

4.1. Sorption mechanism

The adsorption of only net negatively charged monomers and oligomers to the positively charged alumina surface confirmed the importance of electrostatic interaction

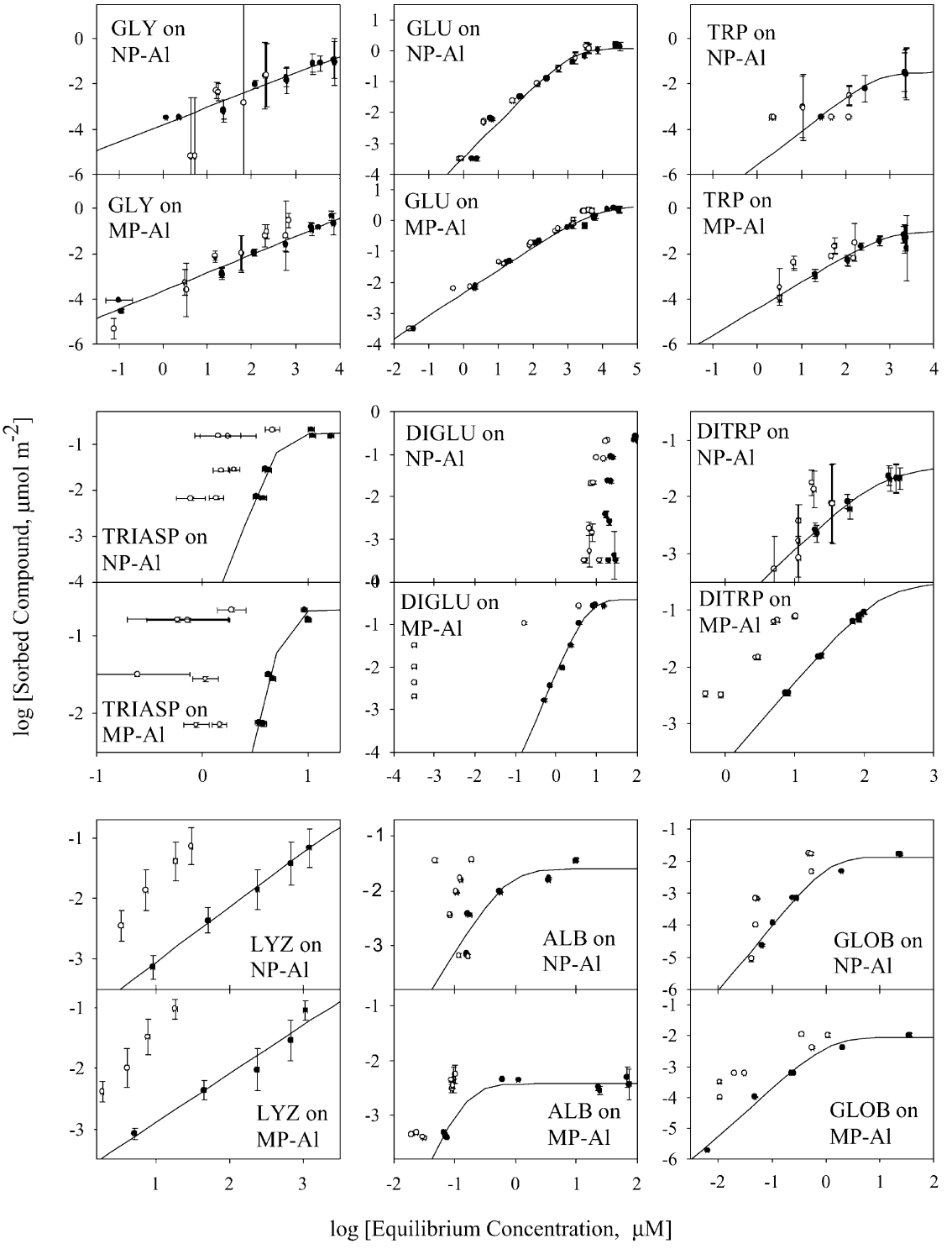

Fig. 1. Adsorption isotherms for amino acids and proteins on nonporous (NP-Al) and mesoporous (MP-Al) alumina. Error bars represent 95% confidence intervals for each data point (difference between two amino acids analyses). Closed circles are adsorption data and open circles are desorption data. Lines are modeled Langmuir–Freundlich adsorption isotherms as described in text.

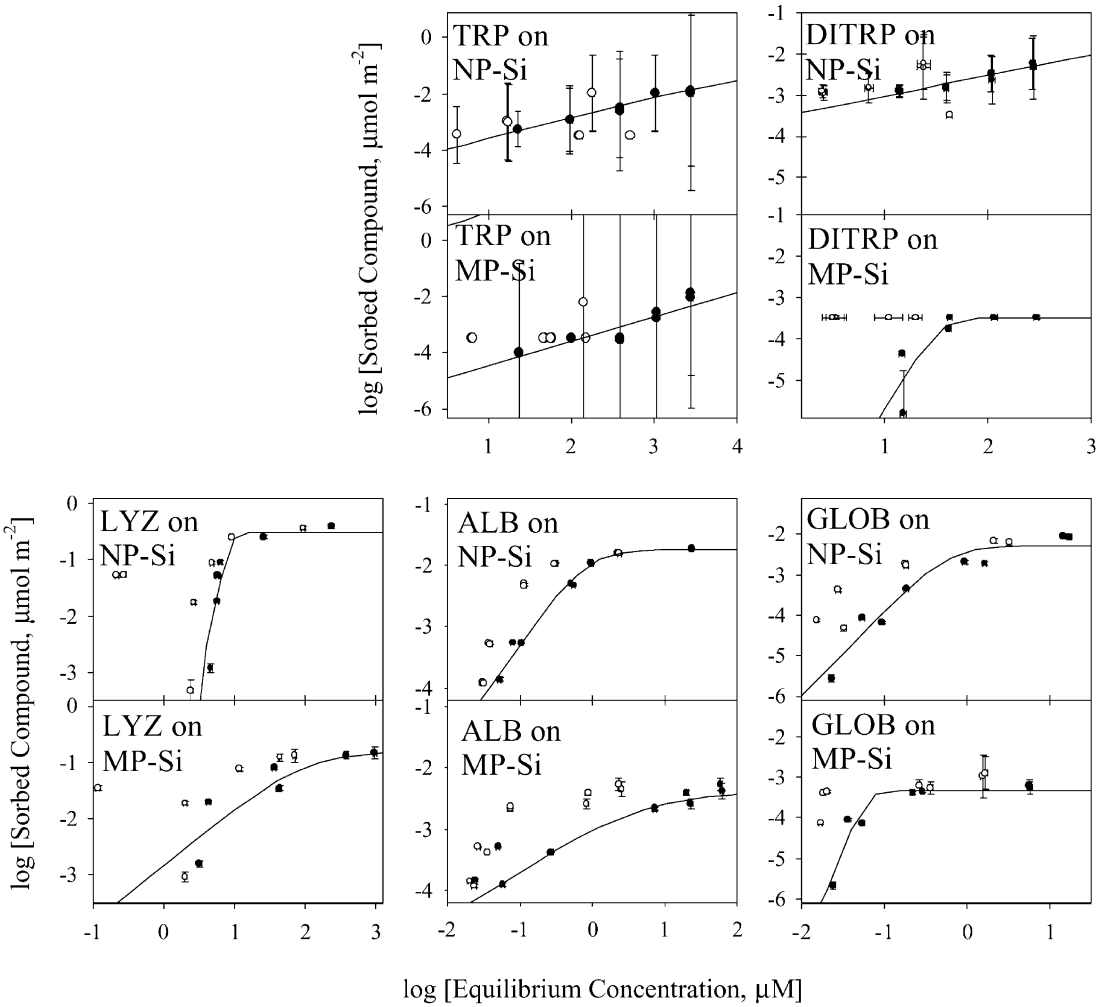

Fig. 2. Adsorption isotherms for amino acids and proteins on nonporous (NP-Si) and mesoporous (MP-Si) silica. Error bars represent 95% confidence intervals for the data point (difference between two amino acids analyses). Closed circle are adsorption points and open circles are desorption points. Lines are modeled Langmuir-Freundlich adsorption isotherms as described in text.

for amino acid adsorption found by others (Rosenfeld, 1979; Hedges and Hare, 1987; Henrichs and Sugai, 1993; Wang and Lee, 1993). Because of this, and because no influence of amino acid loading on the final pH of the solution was observed (data not shown), we hypothesize that the bonding mechanism is predominantly outer-sphere complexation associated with anion exchange rather than inner-sphere complexation associated with ligand exchange. An anion exchange reaction with the alumina surface such as;

$$\equiv \mathrm{AlOH_2^+} - - - \mathrm{Cl^-} + \mathrm{R\text{-}COO^-} \leftrightarrow$$
$$\equiv \mathrm{AlOH_2^+} - - -^- \mathrm{OOC\text{-}R} + \mathrm{Cl^-} \quad (3)$$

is likely and has recently been proposed to describe the adsorption of the contaminant, 2,4-dichlorophenoxyacetic acid to these same alumina materials based on spectroscopic evidence (Goyne, in press). It should be noted, however, that evidence presented by others supports a predominantly inner-sphere complexation-ligand exchange mechanism for adsorption of some organic acids to alumina and clays (McKnight et al., 1992; Ochs et al., 1994; Arnarson and Keil, 2000; Vermohlen et al., 2000).

In contrast to alumina, electrostatic attraction did not control adsorption of amino acid monomers to the silica phases. Instead, only amino acid compounds with hydrophobic moieties sorbed to silica. For this reason, as well as its low surface charge density, it is likely that nonpolar siloxane (Si–O–Si) rather than hydrophilic silanol (Si–OH) are important sites of hydrophobic bonding of amino acids on silica surfaces.

Because of their size, plasticity and multifunctionality, determination of a specific bonding

Table 3
Change in mineral surface area and pore volume with compound adsorption

Sorbent–sorbate pair	% Change surface area[a]	% Change pore volume[a]	Sorbate loading (mg m^{-2})
NP-Al + glycine	−2.2	−1.0	0.25
MP-Al + glycine	−2.4	−5.0	0.27
NP-Al + glutamate	−4.0	6.7	0.22
MP-Al + glutamate	−14.1	−16.5	0.29
NP-Al + ditryptophan	−0.8	14.3	3.3×10^{-3}
MP-Al + ditryptophan	−21.9	−22.8	0.03
NP-Al + albumin	−10.9	14.3	0.76
MP-Al + albumin	−21.0	−29.1	0.19
NP-Al + γ-globlin	−19.7	−12.5	1.88
MP-Al + γ-globlin	−54.6	−55.7	1.46
NP-Si + tryptophan	−3.5	0.0	2.3×10^{-4}
MP-Si + tryptophan	2.4	−6.7	2.3×10^{-4}
NP-Si + albumin	−19.3	0.0	0.27
MP-Si + albumin	−27.9	−25.3	0.13

[a] Percentage difference between control mineral (no sorbed compound) and mineral with sorbed compound, determined by N_2 adsorption as described in text after oven drying (24 h at 60 °C).

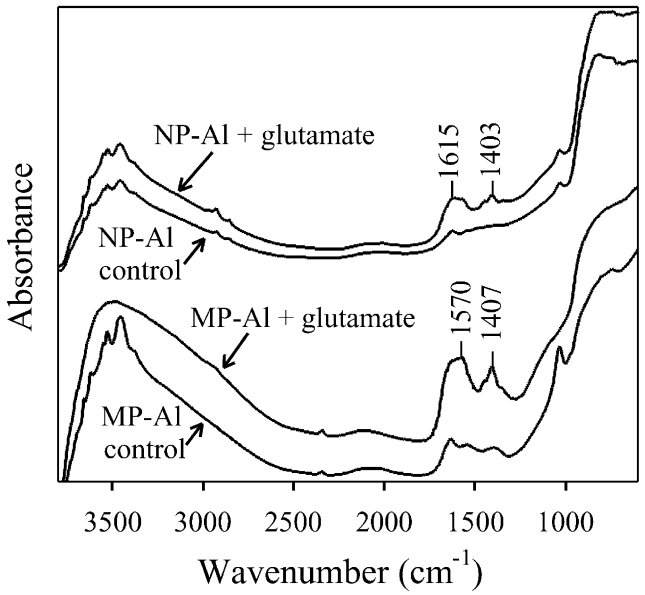

Fig. 3. DRIFT spectra for nonporous (NP-Al) and mesoporous (MP-Al) alumina with sorbed glutamate and with no sorbed compounds (control).

mechanism for proteins adsorbed to surfaces is difficult (Norde, 1986; Arai and Norde, 1990). Although many reactions are possible, hydrogen bonding, electrostatic and hydrophobic interaction are considered most important in driving protein adsorption (Yoon et al., 1996, 1999; Ding and Henrichs, 2002). All the proteins tested in this study sorbed strongly to both alumina and both silica phases, regardless of net charge, suggesting mediation by non-specific hydrophobic attractive interactions such as induced dipole or London dispersive

Table 4
Best fit Langmuir–Freundlich adsorption isotherm parameters[a]

		Alumina sorbent						Silica sorbent					
Sorbate		N	b	m	R^2	K_o	HI_{mn}	N	b	m	R^2	K_o	HI_{mn}
Glycine	NP	1.4	1.1×10^{-4}	0.76	0.95	6.2×10^{-6}	0.9	n.a.[b]	n.a.	n.a.	n.a.	n.a.	n.a.
	MP	26	8.4×10^{-6}	0.80	0.98	4.5×10^{-7}	1.9	n.a.	n.a.	n.a.	n.a.	n.a.	n.a.
Glutamate	NP	1.2	2.7×10^{-4}	1.1	0.97	5.7×10^{-4}	0.6	n.a.	n.a.	n.a.	n.a.	n.a.	n.a.
	MP	3.1	1.4×10^{-3}	0.74	0.99	1.4×10^{-4}	0.5	n.a.	n.a.	n.a.	n.a.	n.a.	n.a.
Diglutamate	NP	0.26	9.0×10^{-4}	1.6	0.34	8.4×10^{-3}	2.4	n.a.	n.a.	n.a.	n.a.	n.a.	n.a.
	MP	0.38	1.6×10^{-2}	2.2	0.99	0.15	6.5×10^{7}	n.a.	n.a.	n.a.	n.a.	n.a.	n.a.
Tryptophan	NP	0.032	7.9×10^{-5}	1.5	1.0	1.8×10^{-3}	0.3	0.088	5.1×10^{-4}	0.74	0.94	3.6×10^{-5}	1.1
	MP	0.094	3.8×10^{-4}	1.2	0.96	1.4×10^{-3}	2.6	2.4	1.9×10^{-6}	0.86	0.83	2.2×10^{-7}	11
Ditryptophan	NP	0.035	2.2×10^{-3}	1.2	0.98	6.1×10^{-3}	2.1	0.15	1.9×10^{-3}	0.50	0.91	3.6×10^{-6}	1.4
	MP	0.31	6.5×10^{-4}	1.4	1.0	5.3×10^{-3}	22	3.2×10^{-4}	3.5×10^{-7}	4.2	0.76	0.03	2.7×10^{6}
Triaspartate	NP	0.17	3.3×10^{-5}	6.0	0.93	0.18	1470	n.a.	n.a.	n.a.	n.a.	n.a.	n.a.
	MP	0.22	2.0×10^{-5}	6.0	0.95	0.16	5.2×10^{6}	n.a.	n.a.	n.a.	n.a.	n.a.	n.a.
Lysozyme	NP	0.90	1.1×10^{-4}	0.92	1.0	5.0×10^{-5}	18	0.31	3.2×10^{-7}	7.1	0.81	0.12	42
	MP	6.5	3.0×10^{-5}	0.80	0.95	2.2×10^{-6}	20	0.15	9.3×10^{-3}	1.0	0.77	0.01	2.5
Albumin	NP	0.025	1.8	1.8	0.85	1.39	12	0.018	1.3	1.7	0.99	1.2	3.2
	MP	0.004	59	2.3	0.96	5.89	6	4.1×10^{-3}	0.29	0.76	0.99	0.20	4.8
γ-Globulin	NP	0.013	0.64	2.0	0.97	0.80	12	0.01	2.6	2.1	0.94	1.6	9.2
	MP	0.009	0.68	1.5	0.99	0.77	18	4.7×10^{-4}	1.8×10^{6}	5.2	0.91	16.0	910

[a] N = LF adsorption capacity (μmol m^{-2}), b = LF binding affinity (μM^{-1}), m = LF heterogeneity index, K_o = LF mean association constant (μM^{-1}), R^2 = correlation coefficient for the model fit to the data, and HI_{mn} = the mean desorption hysteresis index.
[b] n.a. = No adsorption was detected.

forces. The high surface reactivity of proteins on natural sediments has been attributed to these mechanisms by others (Kirchman et al., 1989; Nguyen and Harvey, 2001). While some have concluded that proteins will adsorb to hydrophobic surfaces such as silica under all conditions of charge interaction (Arai and Norde, 1990), other workers (Robinson and Williams, 2002) have observed that significant protein (albumin) adsorption to silica only occurred at higher electrolyte concentrations (> 0.01 M).

4.2. Isotherm modeling

Though most compounds approached a maximum adsorption plateau value at high solution concentrations, the isotherms were poorly modeled by the Langmuir equation perhaps because this model assumes a constant energy of adsorption at all sites. While the Freundlich model does not use this assumption, it assumes an infinite supply of unreacted adsorption sites and cannot, therefore, model saturation behavior. The Langmuir–Freundlich (LF) model behaves as a Freundlich equation at low concentrations and as a Langmuir equation at high solute concentration. This isotherm model has proved successful in modeling a number of other systems involving the adsorption of simple organic compounds and polymers to heterogeneous materials (Yoon et al., 1996; Lee et al., 1998; Kilduff and Wigton, 1999; Li and Werth, 2001; Umpleby et al., 2001).

Of the models tested, the LF model provided the best fit to the data with R^2 values ranging from 0.85 to 1.0 (Table 4). None of the models tested was able to reproduce the isotherm for diglutamate adsorption to NP-Al. The LF parameter N, the adsorption capacity, is in most cases similar to the maximum measured loading. Much higher N parameters, however, were calculated for glycine and lysozyme on both NP-Al and MP-Al, tryptophan on both silica minerals, and ditryptophan on NP-Si. It is clear from this and from the isotherm graphs (Figs. 1 and 2) that maximum adsorption was not reached for these sorbate-sorbent pairs.

While some authors have described the LF parameter m as a heterogeneity index that may only vary from 0 to 1 (Geng and Loh, 2001; Umpleby et al., 2001), with

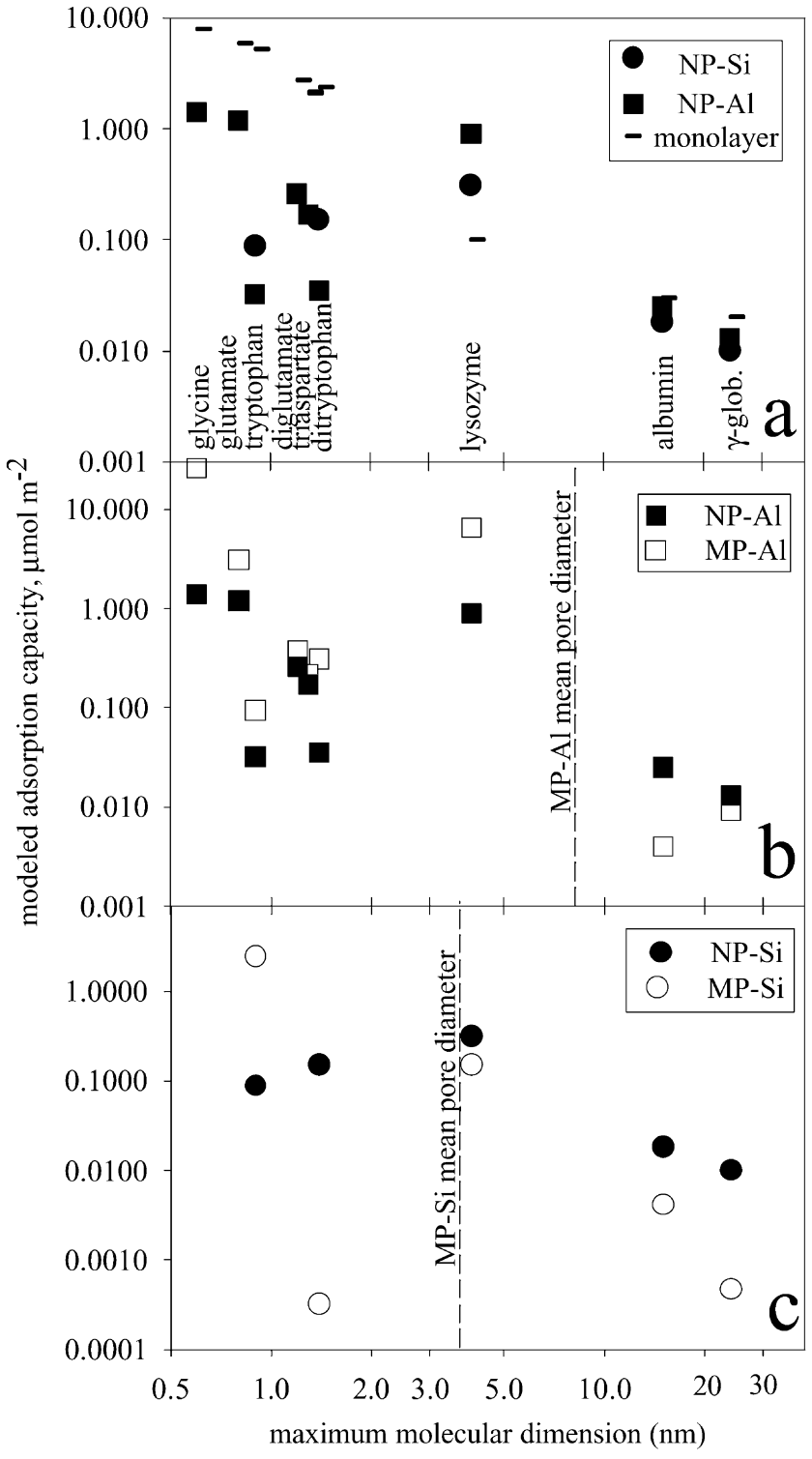

Fig. 4. Comparisons between modeled adsorption capacity parameter (N) versus maximum molecular diameter for compounds sorbed to (a) nonporous alumina versus silica (b) nonporous versus mesoporous alumina and (c) nonporous versus mesoporous silica. Monolayer coverage shown in (a) is calculated by molecular dimension estimates (see text) and assumes cubic closest packing geometry.

Table 5
Comparison of nonporous and mesoporous mineral adsorption capacity at low-medium solution concentration

Sorbate	Equilib. conc.[a] (μM)	LF modeled equilibrium sorbed concentration[b] (μmol m^{-2}) NP-Al	MP-Al	Sorbed conc. MP/NP	Equilib. conc.[b] (μM)	LF modeled equilibrium sorbed concentration[b] (μmol m^{-2}) NP-Si	MP-Si	Sorbed conc. MP/NP
Glycine	10	8.9E-04	1.4E-03	1.6	–	–	–	–
Glutamate	10	4.1E-03	2.4E-02	5.8	–	–	–	–
Diglutamate	10	9.0E-03	2.7E-01	30	–	–	–	–
Tryptophan	10	8.0E-05	5.6E-04	7.1	10	2.5E-04	3.3E-05	0.1
Ditryptophan	10	1.2E-03	5.0E-03	4.2	10	9.0E-04	1.8E-06	0.002
Triaspartate	5	5.8E-02	5.2E-02	0.9	–	–	–	–
Lysozyme	10	8.2E-04	1.2E-03	1.5	5	8.8E-03	6.7E-03	0.8
Albumin	0.1	6.9E-04	9.1E-04	1.3	0.1	4.6E-04	2.0E-04	0.4
γ-Globulin	0.1	8.3E-05	1.9E-04	2.3	0.03	1.6E-05	1.0E-05	0.6

[a] Equilibrium concentration chosen to be in low-medium range of isotherm.
[b] Equilibrium sorbed concentration at chosen solution concentration calculated using LF isotherm.

values near to one indicating an energetically homogeneous surface, others refer to it simply as an exponent related to the heterogeneity of binding site energy distribution and allow it to vary to all positive values (Yoon et al., 1996, 1999; Bautista et al., 2002). We have found that acceptable fits to our adsorption data could not be achieved unless this parameter was allowed to assume values greater than 1. Most *m* values were in the range of 0.5–2.3. Isotherms with higher modeled *m* values, such as for triaspartic acid on both alumina phases and lysozyme and γ-globulin on silica, displayed high slopes at low solution concentration and sharp-edged plateaus. Isotherms such as these may indicate high-affinity attractive forces that disappear as high-energy binding sites are depleted. Binding affinities and heterogeneity indices were generally greater for mesoporous than for nonporous minerals, though no consistent trend could be discerned.

4.3. Comparisons of nonporous phase adsorption capacities

For a given mineral, adsorption capacity expressed on a molar basis generally decreased with sorbate molecular size (Fig. 4) and weight. When expressed on a weight basis, the opposite was true. The hydrophilic amino acid monomer and protein adsorption capacities of NP-Al were about twice that of NP-Si, whereas the adsorption capacities of NP-Si for hydrophobic tryptophan and ditryptophan were 2–3 times greater (Fig. 4a). The adsorption capacities of glycine and glutamate on NP-Al (1.4 and 1.2 μmol m^{-2}, respectively) are similar to the density of positively charged sites at pH 5.7 on NP-Al (1.1 μmol charge m^{-2}; Goyne et al., 2002). In contrast, *N* values for tryptophan and ditryptophan on NP-Si (0.088 and 0.15 μmol m^{-2}, respectively), are well below that mineral's charge density of 0.5 μmol (−) charge m^{-2} (Goyne et al., 2002). These relationships support the proposed bonding mechanisms of predominantly electrostatic interaction (anionic exchange with carboxylate groups) for hydrophilic compounds on alumina and predominantly hydrophobic interaction for hydrophobic compounds on silica. For both NP-Al and NP-Si, modeled amino acid monomer and dimer adsorption capacities are one-fifth (for glycine and glutamate) to two orders of magnitude (for tryptophan and ditryptophan) below a monolayer equivalent coverage based upon closest molecular packing geometry (Fig. 4a). Amino acid monomer and oligomers adsorbed to these nonporous mineral surfaces are, therefore, constrained by surface functionality, i.e. charge and/or hydrophobicity, rather than molecular size.

Other mechanisms contribute to protein adsorption. For example, there is evidence that structural rearrangement occurs during the sorption of proteins (Su et al., 1998; Giacomelli and Norde, 2001) and this breaking of intramolecular bonds causes an increase in entropy that favors sorption (Norde et al., 1986). We observe that protein adsorption capacities closely correspond to a calculated 'closest packing' monolayer, based on globular conformations, for both alumina and silica (Fig. 4a) and are far below these mineral's surface charge densities (Table 1). Further, protein adsorption capacity on nonporous minerals decreases with increasing molecular size.

The adsorption capacities of the proteins on nonporous minerals measured in this study are similar to those reported by others. For example, many workers

have measured maximum sorbed concentrations of albumin on silica in the range 1–3 mg m^{-2} (Norde et al., 1986; Su et al., 1998; Giacomelli and Norde, 2001). Various studies have examined the adsorption of amino acid monomers to sediments and clays (e.g., Dashman and Stotsky, 1982; Henrichs and Sugai, 1993; Wang and Lee, 1993; Naidja and Huang, 1994). However, it is difficult to make comparisons with these studies because experimental conditions such as pH or background electrolyte concentration were not controlled, mineral surface area was not recorded, or OM coatings were not removed.

4.4. Adsorption capacity of mesoporous phases

While adsorption to the mesoporous minerals exhibited the same intermolecular loading trends as the nonporous minerals, we found consistent quantitative differences. All amino acid monomers, oligomers, and lysozyme exhibited greater adsorption capacities on MP-Al versus NP-Al on a surface area-normalized basis (Fig. 4b). In contrast, only tryptophan exhibited a greater adsorption capacity on mesoporous versus nonporous silica (Fig. 4c). The lowest factors of mesopore adsorption capacity enhancement were calculated for diglutamate and triaspartic acid on alumina (1.5 and 1.3, respectively) and the greatest for tryptophan on silica and glycine, lysozyme, and ditryptophan on alumina (27.3, 18.6, 7.2 and 8.9, respectively). The first three of these do not reflect true differences in loadings, however, because they are modeled values and 'plateau' sorbed concentrations were not reached. But the maximum sorbed concentrations of these compounds were also greater for mesoporous versus nonporous minerals analogues (by factors of 1.5–5), measured at equivalent solution equilibrium concentrations. In general, the mesopore enhancement effect was greatest for monomers and decreased with molecular size (or weight), and greater for compounds with hydrophobic moieties. These trends, however, were not consistent.

Both the maximum measured loadings and the calculated adsorption capacities of the two largest proteins, albumin and γ-globulin on MP-Al, were about one-tenth and one-half, respectively, that of NP-Al. Adsorption capacities of all compounds other than tryptophan were greater for NP-Si versus MP-Si by factors ranging from 3 to 20 (Tables 4 and 5). To generalize, adsorption capacities of all compounds of molecular dimensions no larger than about half the pore diameter were greater than that of nonporous minerals. This statement of size constraint should be considered tentative, however, as the most appropriate of the various methods of molecular dimension estimation (including hydrodynamic radii, radius of gyration, static model, and whether to include the sphere of hydration) is unclear. There are additional uncertainties regarding the most appropriate model for the calculation of surface area and pore size by N_2 sorptometry. Lastly, no compounds were tested with molecular dimensions between half and equal to the diameter of the pores.

Post-adsorption experiment BET analyses also indicate that adsorption of organic compounds within mesopores occurred (Table 3). Both surface area and pore volume reductions suggest at least partial filling of the mesopores. These volume reductions cannot, however, be used to evaluate sorption mechanisms since changes in molecular associations must occur upon drying of the samples (see discussion in Goyne et al., in press). To determine whether surface area or pore volume may have constrained MP-Al adsorption capacity, we calculated maximum theoretical compound loadings assuming monolayer coverage or complete pore volume filling (Table 6). These calculations indicate that, while glycine adsorption on MP-Al exceeds monolayer coverage and may be limited, instead, by pore volume, other amino acid compounds do not exceed monolayer or pore-filling capacities of MP-Al or MP-Si. The modeled lysozyme adsorption capacity, however, is greater than both surface area and volume-filling theoretical capacities. In this case, molecular size, adsorption capacity, or the area of sorbate surface occupation may have been overestimated, or multilayer adsorption may have occurred on external mineral surfaces. It is also interesting to note that modeled adsorption capacities of the two largest proteins exceed their theoretical pore volume filling capacity but not their monolayer surface covering capacity.

It is clear that adsorption of compounds larger in size than mesopore diameters was greatly reduced (by factors ranging from 1.4 to 21; Fig. 4) despite similar surface charge densities on the porous and nonporous mineral analogues. For compounds larger than the pores, reduced adsorption capacity of the mesoporous compared to nonporous minerals is consistent with size exclusion from pores. Although sorption onto porous and nonporous minerals has not, to our knowledge, been directly compared, a competitive effect favoring the sorption of smaller over larger nonpolar organic molecules onto microporous materials has been noted. For example, larger sorbates such as atrazine and phenanthrene were excluded from the internal surfaces of soil organic matter relative to smaller molecules such as phenol and trichloroethylene (Xing and Pignatello, 1997; Graber and Borisover, 1998). Similarly, cytochrome *c*, papain and trypsin, but not peroxidase (3, 3.6, 3.8, and 4.6 nm molecular diameter, respectively) could be immobilized within the 4 nm diameter pore openings of a silicate (Diaz and Balkus, 1996). Cytochrome *c* was also excluded from 2.8 nm diameter silicate pores, but, along with pepsin (4-5 nm molecular diameter), was readily sorbed into 13 nm silicate mesopores (Deere et al., 2002). Others have shown similar

protein size restrictions using mesoporous silicates (Kisler et al., 2001; Takahashi et al., 2001; Yiu et al., 2001). In addition, a body of literature exists regarding the adsorption or restriction of organic compounds from pores in activated carbon and polymers from the wastewater treatment and size exclusion chromatography literature, respectively (e.g., Ebie et al., 2001; Geng and Loh, 2001; Vianna-Soares et al., 2002).

4.5. Adsorption affinity

Surface affinity at low to medium sorbate loadings was accessed by calculating the expected sorbed concentration at equilibrium solution concentrations in the positive sloped portions of the isotherms using the LF model. At low equilibrium solution concentrations, surface affinities of all amino acids and proteins except triaspartic acid, were greater for MP-Al versus NP-Al by factors ranging from 1.3 to 30 (Table 5). In contrast all compounds had greater surface affinity for NP-Si versus MP-Si at under-saturated equilibrium solution concentrations. It should be noted, however, that variations in the chemistry of binding sites, as indicated by the differences in binding site heterogeneity, m, of the various materials, may lead to some of the differences observed in loadings at these lower equilibrium solution concentrations.

In order to examine possible changes in sorbate-sorbent affinity with increased sorbate loadings, adsorption affinity distributions were calculated for each sorbate-sorbent pair. Six representative distributions are shown in Fig. 5. All the affinity distributions calculated for the compounds examined in this study were assumed to be unimodal and symmetrical. The mean association constant for each sorbent-sorbate pair ($K_o = b^{1/m}$; Table 4), therefore, corresponds to the association constant (K) of the maximum number of bonding sites or the mode of the affinity distribution (Umpleby et al., 2001). Although this model should be treated as semi-empirical because it assumes a simple and uniform energy distribution, a few generalizations can be made.

K_o tends to increase with the molecular weight of the compound bound to a given phase. The height of the mode of the affinity distribution corresponds to the modeled adsorption capacity and is greater for compounds sorbed to MP phases versus their NP analogues as previously discussed. In nearly all cases in which compounds were not inhibited from entering pores due to molecular size constraints, affinity spectra peaks are shifted to lower K values and broadened when sorbed to the MP phases (Fig. 5a and b). This was true for all compounds except for diglutamate sorbed to alumina. Peak broadening is an indication of greater heterogeneity which can be attributed to a diversity of bonding site energies or to a diversity of binding mechanisms due to the presence of mesoporosity. The shift to the left suggests that, at higher sorbate concentrations, the additional sorbate-sorbent interactions with mesoporous material are not as strong as those on the nonporous minerals on average. In contrast, larger compounds that are unable to enter pores exhibit similar distributions whether sorbed to porous or nonporous phases (Fig. 5c).

While some have ascribed surface energy heterogeneity to pore structure and size distribution alone (Geng and Loh, 2001), correspondence between experimental conditions such as pH and solvent type and affinity distribution (Yoon et al., 1996; Geng and Loh, 2001) indicates that sorption mechanism must play a significant role. In addition, modeling has shown that compounds of varying size interact differently with energetically heterogeneous surfaces (Dabrowski and Jaroniec, 1987), a finding that is consistent our data.

4.6. Desorption hysteresis

Desorption hysteresis was quantified by calculating a hysteresis index for each sorbate–sorbent pair. With the exception of glutamate sorbed to alumina that exhibited no hysteresis, all amino acid monomers and dimers exhibited greater HI_{mn} values for mesoporous versus nonporous mineral sorbents (Table 4). Hysteresis was enhanced by factors of 2–10 for amino acid monomers and 10^3–10^6 for dimers and trimers on mesoporous versus nonporous minerals. While all proteins examined exhibited desorption hysteresis, there were no consistent trends in HI_{mn} values for mesoporous versus nonporous analogs. Apart from lysozyme sorbed to MP-Al, other evidence does not indicate the adsorption of these proteins to the internal surfaces of mesopores. Nevertheless, surface heterogeneity, multiple points of attachment, the presence of micropores, post-adsorption molecular rearrangements, or some other factor as yet unconsidered, apparently leads to desorption hysteresis in the cases of proteins.

4.7. Mesopore adsorption mechanism

Although enhanced adsorption of gases within micropores has long been recognized (Everett and Powl, 1975), a mechanism for enhanced adsorption of organic compounds onto mesoporous minerals is not obvious. While theory describing the adsorption of gases to heterogeneous microporous and mesoporous materials exists (see Rudzinski and Everett, 1992), less work has been done describing the adsorption of organic compounds to mesoporous materials. Such a mechanism must explain the enhanced adsorption, reduced desorption, increased adsorption affinities at low sorbate loadings and decreased adsorption affinities at high sorbate loadings that we measure for most compounds that sorb to mesopore internal surfaces. A

Table 6
Experimental and theoretical maximum adsorption capacity

	Modeled adsorption capacity, N		Monolayer loading[a] (μmol m^{-2})	Filled-pore volume loading[a] (μmol m^{-2})	Modeled adsorption capacity, N		Monolayer loading[a] (μmol m^{-2})	Filled-pore volume loading[a] (μmol m^{-2})
	(μmol m^{-2})	(mg m^{-2})			(μmol m^{-2})	(mg m^{-2})		
Sorbate	MP-Al sorbent (+1.0 μmol charge m^{-2})				MP-Si sorbent (−0.25 μmol charge m^{-2})			
Glycine	26	1.5	7.91	32.7	—	—	7.91	17.1
Glutamate	3.1	0.40	5.93	18.4	—	—	5.93	9.64
Diglutamate	0.38	0.11	2.77	5.72	—	—	2.77	2.30
Tryptophan	0.09	0.017	5.93	18.4	2.4	0.45	5.93	9.64
Ditryptophan	0.31	0.12	2.37	4.20	0.0003	0.0001	2.37	2.20
Triaspartate	0.22	0.080	2.31	4.76	—	—	2.31	2.50
Lysozyme	6.5	92.95	0.14	0.114	0.15	2.15	0.14	0.060
Albumin	0.004	0.26	0.03	0.005	0.004	0.27	0.03	0.002
γ-Globulin	0.009	1.52	0.02	0.002	0.0005	0.079	0.02	0.001

[a] Based on BET-calculated surface area and pore volume. Assumes major×minor axis as molecular area, major×major×minor axis as molecular volume, globular molecular conformation and cubic symmetry packing.

number of possible mechanisms could explain at least some of these observations.

Increased attractive interaction between compounds sorbed to internal mesopore surfaces in monolayer or near monolayer coatings may occur due to surface curvature that brings unbound moieties closer together (Farrell and Reinhard, 1994). This mechanism has been invoked to explain enhanced adsorption of 2,4-dichlorophenoxyacetic acid to mesoporous alumina (Goyne et al., in press). We do not favor this mechanism for phenomena described here because one would not expect all the compounds tested in this study to exhibit self-attraction, particularly those with a high net charge such as triaspartic acid. Additionally, many of the compound loadings do not approach monolayer coverage.

Increased attractive sorbate-sorbent interaction may be caused by curvature or roughness of pore walls. As pointed out by Farrell and Reinhard (1994), due to the superposition of interaction potentials on opposing pore walls, adsorption energies should be greatly increased within pores. Interaction potentials have been calculated to be significantly increased for noble gases sorbed within micropores up to three molecular-diameters in size (Everett and Powl, 1975). Alternatively, it is plausible that surface curvature or increased defect structures might favor the formation of bidentate or bridging bonds between sorbent and sorbate relative to monodentate bonds that might be favored on a flat mineral surface. This mechanism is consistent with the downward frequency shift in the asymmetric carboxylate vibration associated with the adsorption of glutamate and diglutamate to MP-Al relative to NP-Al (Fig. 3). However, this shift was not observed for all compounds tested. Goyne et al. (in press) have shown that this effect may be an artifact of freeze-drying because they did not observe the same shifts when wet samples were examined by attenuated total reflectance-Fourier transform infrared (ATR-FTIR). Further, the absence of hydroxyl release upon sorption suggests outer-sphere bonding and our models indicate decreased rather than increased adsorption bond energies for mesopore-bonded compounds at high loading rates. For these reasons, we do not favor this mesopore adsorption-enhancement mechanism.

Polymerization of compounds might be enhanced within pores such that their exit from pores is hindered by size constraints or steric considerations. Some have observed polymerization of amino acids sorbed to mineral surfaces including alumina and silica gel (e.g., Ferris et al., 1996; Bujdak and Rode, 1999, 2002; Ogawa et al., 1999). These experiments have led to the hypothesis that minerals may have catalyzed the formation of the first prebiotic peptides. Though the influence of surface morphology on polymerization has not been explored experimentally, some have hypothesized that the first cells may have originated within mineral mesopores (Smith et al., 1999). Experiments observing mineral-catalyzed polymerization, however, were carried out using specific conditions such as multiple wetting/drying cycles, high temperatures or the addition of condensing agents. We extracted organic matter from the MP-Al and MP-Si minerals following adsorption experiments with glycine, glutamate and tryptophan. High pressure liquid chromatography (HPLC) analysis

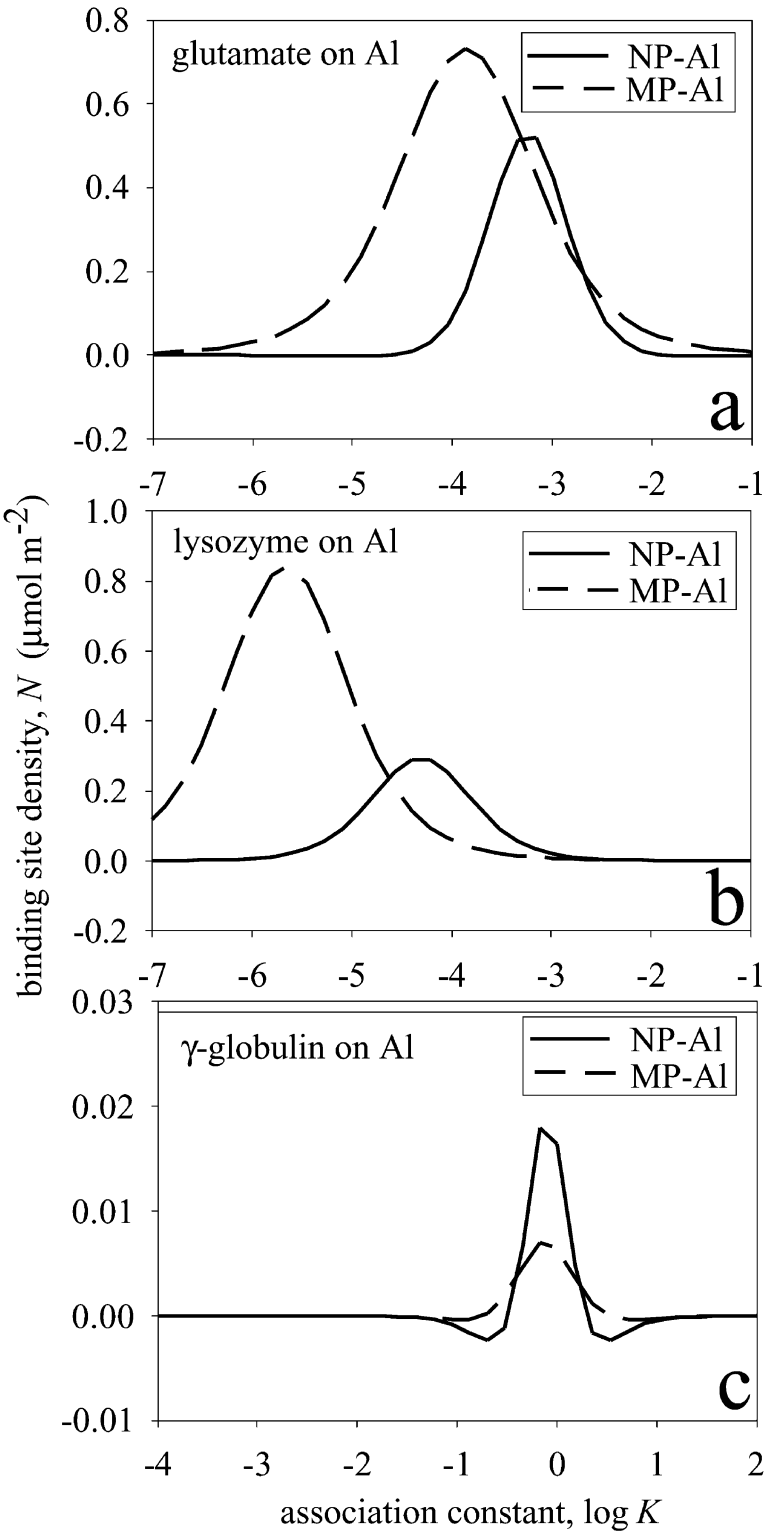

Fig. 5. Affinity distributions; binding sites density, N, versus log of association constant K for (a) glutamate, (b) lysozyme and (c) γ-globulin, sorbed to nonporous (NP-Al) and mesoporous (MP-Al) alumina.

of the extracts revealed no evidence of the formation of dimers or oligomers from these monomers. Further, while this mechanism may explain the observed slower rates of desorption (hysteresis), it cannot explain the greater adsorption capacity of mesoporous surfaces.

Adsorption may be affected by chemical or physical changes in the aqueous layer adjacent to the mineral surface due to mesopore containment. For example, partitioning of nonpolar compounds into vicinal water, a highly order layer of water within a few nanometers of the mineral surface (Schwarzenbach et al., 1993), may be enhanced by strong force fields within pores. Wang et al. (2002) have noted enhanced adsorption of ions (H^+, OH^-, and Zn^+) on mesoporous versus nonporous alumina in both experiments and models. These results were attributed to overlap of the electric double layer (EDL) within pores leading to greater surface charge density. This mechanism might explain the increased adsorption affinities that we measure at low sorbent loadings on MP-Al relative to NP-Al. It would also provide an explanation for the absence of this effect for the more hydrophobic silica surface. Arguing against this mechanism, we measured no difference between the surface charge densities of MP-Al and NP-Al at the experimental pH (Goyne et al., 2002). At 0.02 M, the ionic strength of our experiments, one can calculate an EDL thickness of about 2 nm. In the 8.2 nm diameter pores of MP-Al used here, one would not expect a great deal of EDL overlap unless the pores are slit-shaped. Measurements of sorption enthalpies led Farrell et al. (1999) to conclude that, for trichloroethylene, sorption into vicinal water within micropores was not a predominant sorption mechanism. Lastly, one would not expect these mechanisms to be effective for a wide range of compound types including hydrophilic and hydrophobic amino acids and small proteins. EDL overlap may play a role in the enhanced adsorption of organic compounds in mesopores but cannot explain all of our experimental observations.

Pore-filling has been proposed to explain the non-linear isotherms (Xing and Pignatello, 1997; Kleineidam et al., 2002) and enhanced adsorption of nonpolar and low-polarity organic compounds (Xing et al., 1996; Xia and Ball, 1999) often observed during sorption into micropores. This mechanism is somewhat analogous to the capillary condensation of gases within mesopores that is mathematically described by the BJH method (Barrett et al., 1951) and is used to calculate pore volume by N_2 adsorption. Capillary condensation occurs as multilayers are deposited from opposing walls and is characterized by enhanced sorbent uptake at low relative vapor pressures due to the presence of strong force fields near pore walls (Webb and Orr, 1997). Desorption hysteresis occurs because evaporation occurs at lower relative pressures than condensation because of the presence of a curved meniscus (Webb and Orr, 1997). Solute adsorption within pores presents an analogous situation in that the aqueous solubility of a solute molecule is relatively decreased due to the increase in interfacial area during desorption (Farrell et al., 1999).

We favor a pore-filling mechanism to explain the majority of our experimental observations. It explains the decreases in pore areas and volumes following adsorption experiments (Table 3). Because pores needn't be completely filled, loading capacities less than that of a theoretical monolayer or a filled pore (Table 5) are acceptable. While EDL overlap or increased sorbate-sorbent interaction may be invoked to explain the relatively increased adsorption affinities at low sorbent loadings on MP-Al (Table 6), pore-filling may explain the apparently decreased sorption affinities at higher sorbate loadings (Fig. 5). As pores fill, higher energy sorbent-sorbate interaction sites become occupied and lower strength sorbate-sorbate interactions begin to occur. For example, the appearance of a low energy peak during N_2 adsorption to a silica gel was attributed to the onset of multilayer adsorption whereas higher energy peaks were related to interactions at the silica surface (Puziy et al., 2003).

Desorption may be inhibited by the creation of a hydrophobic nanoenvironment (Farrell and Reinhard, 1994) within the confined environment of a mesopore where hydration spheres may be collapsed or water excluded. We observed that compounds with some hydrophobicity display a greater degree of hysteresis. Hanna et al. (2002) measured increasing sorption into silica mesostructures along a series of organic compounds with increasing hydrophobicity. For hydrophilic compounds, attraction may be enhanced by hydrogen-bonding, electrostatic or ion-dipole interaction within mesopores. It should be noted that some of the above mechanisms may operate in tandem. More focused study of the bonding mechanism for organic matter within mesopores is clearly needed.

5. Conclusions

While the mechanistic details of mesopore sorption remain to be further studied, it is clear that amino acid and small protein compounds may be strongly 'bound' within mesopores and undergo reduced desorption. Further, larger proteins, such as those the size of most enzymes, are excluded from the pores. The 'mesopore protection hypothesis' is, therefore a feasible preservation mechanism for soil and sedimentary environments. This mechanism will more effectively preserve hydrophobic compounds or compounds with hydrophobic moieties that are less readily desorbed from mesopores. This may partly explain the preferential preservation of these types of compounds in soils and sediments. This

study indicates, however, that even hydrophilic compounds may be sequestered within mineral mesopores. While these experiments were carried out in model systems, and soils and sediment are much more heterogeneous with a wide range of pore sizes and mineral types, these results demonstrate the possible importance of mesopores in controlling the preservation and fractionation of both natural organic matter and organic contaminants.

Acknowledgements

We thank Bharat Newalkar of the Materials Research Laboratory, The Pennsylvania State University for production of the mesoporous phases, Mary Kay Amistadi, University of Arizona, for assistance with DRIFT analyses, and James Kubicki, Penn State Department of Geosciences, for assistance with molecular modeling. We also appreciate the helpful suggestions of Drs. Larry Mayer and Karen Wilson in their review of this manuscript. This research was partially supported by the Penn State Biogeochemical Research Initiative for Education (BRIE) sponsored by NSF (IGERT) grant DGE-9972759, Materials Research Science and Engineering Center (MRSEC) under grant DMR 0213623 (for S.K.). Acknowledgment is also made to the donors of the American Chemical Society Petroleum Research Fund for partial support of this research.

Associate Editor—**B. Keely**

References

Anbeek, C., Vanbreeman, N., Meijer, E., Vanderplas, L., 1994. The dissolution of naturally weathered feldspar and quartz. Geochimica et Cosmochimica Acta 58, 4601–4613.

Arai, T., Norde, W., 1990. The behavior of some model proteins at solid-liquid interfaces 1. Adsorption from single protein solutions. Colloids and Surfaces 51, 1–15.

Arnarson, T.S., Keil, R.G., 2000. Mechanisms of pore water organic matter adsorption to montmorillonite. Marine Chemistry 71, 309–320.

Baham, J., Sposito, G., 1994. Adsorption of dissolved organic carbon extracted from sewage sludge on montmorillonite and kaolinite in the presence of metal ions. Journal of Environmental Quality 23, 147–153.

Baldock, J.A., Skjemstad, J.O., 2000. Role of soil matrix and minerals in protecting natural organic materials against biological attack. Organic Geochemistry 31, 697–710.

Ball, W., Buehler, C.H., Harmon, T.C., MacKay, D.M., Robert, P.V., 1990. Characterization of a sandy aquifer material at the grain scale. Journal of Contaminant Hydrology 5, 253–295.

Barrett, E.P., Joyner, L.G., Halenda, P.P., 1951. The determination of pore volume and area distributions in porous substances. I. Computations from nitrogen isotherms. Journal of the American Chemical Society 73, 373–380.

Bautista, L.F., Pinilla, J., Aracil, J., Martinez, M., 2002. Adsorption isotherms of aspartame on commercial and chemically modified divinylbenzene-styrene resins at different temperatures. Journal of Chemical & Engineering Data 47, 620–627.

Bergamaschi, B.A., Tsamakis, E., Keil, R.G., Eglinton, T.I., Montlucon, D.B., Hedges, J.I., 1997. The effect of grain size and surface area on organic matter, lignin, carbohydrate concentration, and molecular composition in Peru Margin sediments. Geochimica et Cosmochimica Acta 61, 1247–1260.

Bock, M.J., Mayer, L.M., 2000. Mesodensity organo-clay associations in a near-shore sediment. Marine Geology 163, 65–75.

Boyd, S.A., Mortland, M., 1996. Enzyme interactions with clays and clay-organic matter complexes. In: G. Stotzky, J.-M. Bollag (Eds.), Soil Biochemistry, Vol. 9, pp. 1.

Brantley, S.L., Mellot, N.P., 2000. Surface area and porosity of primary silicate minerals. American Minerologist 85, 1767–1783.

Brantley, S.L., White, A.F., Hodson, M.E., 1999. Surface area of primary silicate minerals. In: Jamtveit, B., Meakin, P. (Eds.), Growth, Dissolution and Pattern Formation in Geosystems. Kluwer Academic Publishers, The Netherlands, pp. 291–326.

Brunauer, S., 1943. The Adsorption of Gases and Vapors. Vol. I, Physical Adsorption. Princeton University Press, Princeton, NJ.

Brunauer, S., Emmet, P.H., Teller, E., 1938. Adsorption of gases in multimolecular layers. Journal of the American Chemical Society 60, 309.

Bujdak, J., Rode, B.M., 1999. Silica, alumina, and clay catalyzed peptide bond formation: enhanced efficiency of alumina catalyst. Origins of Life and Evolution of the Biosphere 29, 451–461.

Bujdak, J., Rode, B.M., 2002. Preferential amino acid sequences in alumina-catalyzed peptide bond formation. Journal of Inorganic Biochemistry 90, 1–7.

Chorover, J., Amistadi, M.K., 2001. Reaction of forest floor organic matter at goethite, birnessite, and smectite surfaces. Geochimica et Cosmochimica Acta 65, 95–109.

Collins, M.J., Bishop, A.N., Farrimond, P., 1995. Sorption by mineral surfaces: rebirth of the classical condensation pathway for kerogen formation? Geochimica et Cosmochimica Acta 59, 2387–2391.

Confer, D.R., Logan, B.E., Aiken, B.S., Kirchman, D.L., 1995. Measurement of dissolved free and combined amino acids in unconcentrated wastewaters using high performance liquid chromatography. Water Environment Research 67, 118–125.

Dabrowski, A., Jaroniec, M., 1987. Theoretical foundations of physical adsorption from binary non-electrolytic liquid mixtures on solid surfaces: present and future. Advances in Colloid and Interface Science 27, 211–283.

Dashman, T., Stotsky, G., 1982. Adsorption and binding of amino acids on homoionic montmorillonite and kaolinite. Soil Biology and Biochemistry 14, 447–456.

de Jonge, H., Mittelmeijer-Hazeleger, M.C., 1996. Adsorption of CO_2 and N_2 on soil organic matter: nature of porosity,

surface area, and diffusion mechanisms. Environmental Science and Technology 30, 408–413.

Deere, J., Magner, E., Wall, J.G., Hodnett, B.K., 2002. Mechanistic and structural features of protein adsorption onto mesoporous silicates. Journal of Physical Chemistry B 106, 7340–7347.

Diaz, J.F., Balkus Jr., K.J., 1996. Enzyme immobilization in MCM-41 molecular sieve. Journal of Molecular Catalysis B: Enzymatic 2, 115–126.

Ding, X., Henrichs, S.M., 2002. Adsorption and desorption of proteins and polyamino acids by clay minerals and marine sediments. Marine Chemistry 77, 225–237.

Ebie, K., Li, F.S., Azuma, Y., Yuasa, A., Hagishita, T., 2001. Pore distribution effect of activated carbon in adsorbing organic micropollutants from natural water. Water Research 35, 167–179.

Everett, D.H., Powl, J.C., 1975. Adsorption in slit-like and cylindrical micropores in the Henrey's Law region. Journal of the Chemical Society. Faraday Transactions I 1976, 619–636.

Farrell, J., Hauck, B., Jones, M., 1999. Thermodynamic investigation of trichloroethylene adsorption in water-saturated microporous adsorbents. Environmental Toxicology and Chemistry 18, 1637–1642.

Farrell, J., Reinhard, M., 1994. Desorption of halogenated organics from model solids, sediments, and soil under unsaturated conditions. 1. Isotherms. Environmental Science and Technology 28, 53–62.

Ferris, J.P., Hill Jr., A.R., Liu, R., Orgel, L.E., 1996. Synthesis of long prebiotic oligomers on mineral surfaces. Nature 381, 59–61.

Geng, A., Loh, K.-C., 2001. Heterogenity of surface energies in reverse-phase perfusive packings. Journal of Colloid and Interface Science 239, 447–457.

Giacomelli, C.E., Norde, W., 2001. The adsorption-desorption cycle. Reversibility of the BSA-silica system. Journal of Colloid and Interface Science 233, 234–240.

Goyne, K.W., Brantley, S.L., Zimmerman, A.R., Komarneni, S., Chorover, J. Influence of mesoporosity on the sorption of 2,4-dichlorophenoxyacetic acid to alumina and silica. Journal of Colloid and Interface Science (in press).

Goyne, K.W., Zimmerman, A.R., Newalkar, B.L., Komarneni, S., Brantley, S.L., Chorover, J., 2002. Surface charge of variable porosity Al_2O_3 (s) and SiO_2 (s) adsorbents. Journal of Porous Materials 9, 243–256.

Graber, E.R., Borisover, M.D., 1998. Hydration-facilitated sorption of specifically interacting organic compounds by model soil organic matter. Environmental Science and Technology 32, 258–263.

Gu, B., Schmitt, J., Chen, Z., Liang, L., McCarthy, J.F., 1994. Adsorption and desorption of natural organic matter on iron oxide: mechanisms and models. Environmental Science and Technology 28, 38–46.

Gu, B., Schmitt, J., Chen, Z., Liang, L., McCarthy, J.F., 1995. Adsorption and desorption of different organic matter fractions on iron oxide. Geochimica et Cosmochimica Acta 59, 219–229.

Halsey, G., 1948. Physical adsorption on non-uniform surfaces. Journal of Chemical Physics 16, 931.

Hanna, K., Beurroies, I., Denoyel, R., Desplantier-Giscard, D., Galarneau, A., Di Renzo, F., 2002. Sorption of hydrophobic molecules by organic/inorganic mesostrucures. Journal of Colloid and Interface Science 252, 276–283.

Harms, H., Bosma, T.N.P., 1996. Mass transfer limitation of microbial growth and pollutant degradation. Journal of Industrial Microbiology 16, 1–9.

Hedges, J.I., Hare, P.E., 1987. Amino acid adsorption by clay minerals in distilled water. Geochimica et Cosmochimica Acta 51, 255–259.

Hedges, J.I., Keil, R.G., 1995. Sedimentary organic matter preservation: an assessment and speculative synthesis. Marine Chemistry 49, 81–115.

Henrichs, S.M., Sugai, S.F., 1993. Adsorption of amino acids and glucose by sediments of Resurrection Bay, Alaska, USA: functional group effects. Geochimica et Cosmochimica Acta 57, 823–835.

Hodson, M.E., 1998. Micropore surface area variation with grain size in unweathered alkali feldspars; implications for surface roughness and dissolution studies. Geochimica et Cosmochimica Acta 62, 3429–3435.

Huang, W., Peng, P., Yu, Z., Fu, J., 2003. Effects of organic matter heterogeneity on sorption and desorption of organic contaminants by soils and sediments. Applied Geochemistry 18, 955–972.

Huang, W., Weber Jr., W.J., 1997. A distributed reactivity model for sorption by soils and sediments. 10. Relationships between desorption, hysteresis, and the chemical characteristics of organic domains. Environmental Science and Technology 31, 2562–2569.

Huang, W., Yu, H., Weber Jr., W.J., 1998. Hysteresis in the sorption and desorption of hydrophobic organic contaminants by soils and sediments 1. A comparitive analysis of experimental protocols. Journal of Contaminant Hydrology 31, 129–148.

Hulthe, G., Hulth, S., Hall, P.O.J., 1998. Effect of oxygen on degradation rate of refractory and labile organic matter in continental margin sediments. Geochimica et Cosmochimica Acta 62, 1319–1328.

Jardine, P.M., Weber, N.L., McCarthy, J.F., 1989. Mechanisms of dissolved organic carbon adsorption on soil. Soil Science Society of America Journal 53, 1378–1385.

Jastrow, J.D., Miller, R.M., 1997. Soil Aggregate Stabilization and Carbon Sequestration: Feedbacks Through Organo-Mineral Associations. CRC Press, Boca Raton, FL.

Kaiser, K., Guggenberger, G., 2000. The role of DOM sorption to mineral surfaces in the preservation of organic matter in soils. Organic Geochemistry 31, 711–725.

Keil, R.G., 1994. Sorptive preservation of labile organic matter in marine sediments. Nature 370, 549–552.

Kennedy, M.J., Pevear, D.R., Hill, R.J., 2002. Mineral surface control of organic carbon in black shale. Science 259, 657–660.

Kilduff, J.E., Wigton, A., 1999. Sorption of TCE by humic-preloaded activated carbon: Incorporating size-exclusion and pore-blockage phenomena in a competitive adsorption model. Environmental Science & Technology 33, 250–256.

Kirchman, D.L., Henry, D.L., Dexter, S.C., 1989. Adsorption of proteins to surfaces in seawater. Marine Chemistry 27, 201–217.

Kisler, J.M., Dahler, A., Stevens, G.W., O'Conner, A.J., 2001. Separation of biological molecules using mesoporous molecular sieves. Microporous and Mesoporous Materials 44- 45, 769–774.

Kleineidam, S., Scuth, C., Grathwohl, P., 2002. Solubility-normalized combined adsorption-partitioning sorption isotherms for organic pollutants. Environmental Science and Technology 36, 4689–4697.

Komarneni, S., Pidugu, R., Menon, V., 1996. Water adsorption and desorption isotherms of silica and alumina mesoporous molecular sieves. Journal of Porous Minerals 3, 99–106.

Kostoglod, N., Sychev, M., Prikhod'ko, R., Astrelin, I., Stepanenko, A., Rozwadowski, M., 1998. Porous structure of pillared clays. II. Montmorillonite pillared with titanium dioxide. Kinetics and Catalysis 39, 547–553.

Langmuir, I., 1916. The constitution and fundamental properties of solids and liquids. Journal of the American Chemical Society 38, 2221–2295.

Lee, J.H., Yoon, J.-Y., Kim, W.-S., 1998. Continuous separation of serum proteins using a stirred cell charged with carboxylated and sulfonated microspheres. Biomedical Chromatography 12, 330–334.

Li, J., Werth, C.J., 2001. Evaluating competitive sorption mechanisms of volatile organic compounds in soils and sediments using polymers and zeolites. Environmental Science and Technology 35, 568–574.

Lindroth, P., Mopper, K., 1979. High performance liquid chromatographic determination of subpicomolar amounts of amino acids by precolumn fluorescence derivitization with o-phthaldialdehyde. Analytical Chemistry 51, 1667–1674.

Luthy, R.G., Aiken, G.R., Brusseau, M.L., Cunningham, S.D., Gschwend, P.M., Pignatello, J.J., Reinhard, M., Traina, S.J., Weber Jr., W.J., Westall, J.C., 1997. Sequestration of hydrophobic organic contaminants by geosorbents. Environmental Science and Technology 31, 3341–3347.

Malekani, K., Rice, J.A., Lin, J.S., 1997. The effect of sequential removal of organic matter on the surface morphology of humin. Soil Science 165, 333–342.

Mayer, L.M., 1994a. Relationship between mineral surfaces and organic carbon concentration in soils and sediments. Chemical Geology 114, 347–363.

Mayer, L.M., 1994b. Surface area control of organic carbon accumulation in continental shelf sediments. Geochimica et Cosmochimica Acta 58, 1271–1284.

Mayer, L.M., 1999. Extent of coverage of mineral surfaces by organic matter in marine sediments. Geochimica et Cosmochimica Acta 63, 207–215.

Mayer, L.M., Macko, S.A., Cammen, L., 1988. Provenance, concentration and nature of sedimentary organic nitrogen in the Gulf of Maine. Marine Chemistry 25, 291–304.

McKnight, D.M., Bencala, K.E., Zellweger, G.W., Aiken, G.R., Feder, G.L., Thorn, K.A., 1992. Sorption of dissolved organic carbon by hydrous aluminum and iron oxides occurring at the confluence of Deer Creek with the Snake River, Summit County, Colorado. Environmental Science and Technology 26, 1388–1396.

Moore, T.R., 1997. Dissolved Organic Carbon: Sources, Sinks, Fluxes, and Role in the Soil Carbon Cycle. CRC Press, Boca Raton.

Naidja, A., Huang, P.M., 1994. Aspartic acid interaction with Ca-montmorillonite: adsorption, desorption and thermal stability. Applied Clay Science 9, 265–281.

Neaman, A., Pelletier, M., Villieras, F., 2003. The effects of exchanged cation, compression, heating and hydration on textural properties of bulk bentonite and its corresponding purified montmorillonite. Applied Clay Science 22, 153–168.

Nguyen, R.T., Harvey, H.R., 2001. Preservation of protein in marine systems: hydrophobic and other noncovalent associations as major stabilizing forces. Geochimica et Cosmochimica Acta 65, 1467–1480.

Norde, W., 1986. Adsorption of proteins from solution at the solid-liquid interface. Advances in Colloid and Interface Science 25, 267–340.

Norde, W., MacRitchie, F., Nowicka, G., Lyklema, J., 1986. Protein adsorption at solid-liquid interfaces: reversibility and conformation aspects. Journal of Colloid and Interface Science 112, 447–456.

Ochs, M., Cosovic, B., Stumm, W., 1994. Coordinative and hydrophobic interaction of humic substances with hydrophilic Al_2O_3 and hydrophobic mercury surfaces. Geochimica et Cosmochimica Acta 58, 639–650.

Ogawa, H., Fujigaki, T., Chihara, T., 1999. Selective formation of glycylglycine by dehydration of glycine adsorbed on silica gel. Journal of Physical Organic Chemistry 12, 354–356.

Pennell, K.D., Boyd, S.A., Abriola, L.M., 1995. Surface area of soil organic matter reexamined. Soil Science Society of America Journal 59, 1012–1018.

Puziy, A.M., Charmas, B., Puddubnaya, O.I., Mel'gunov, M.S., Leboda, R., Trznadel, B.J., 2003. Surface heterogeneity of carbon-silica adsorbents studied on the basis of the complex adsorption investigations. Colloids and Surfaces A: Physicochemical and Engineering Aspects 213, 45–57.

Ransom, B., Bennett, R.H., Baerwald, R., Shea, K., 1997. TEM study of in situ organic matter on continental margins: occurrence and the "monolayer" hypothesis. Marine Geology 138, 1–9.

Riboulleau, A., Mongenot, T., Baudin, F., Derenne, S., Largeau, C., 2002. Factors controlling the survival of proteinaceous material in Late Tithonian kerogens (Kashpir Oil Shales, Russia). Organic Geochemistry 33, 1127–1130.

Robinson, S., Williams, P.A., 2002. Inhibition of protein adsorption onto silica by polyvinylpyrrolidone. Langmuir 18, 8743–8748.

Rockne, K.J., Taghon, G.L., Kosson, D.S., 2000. Pore structure of soot deposits from several combustion sources. Chemosphere 41, 1125–1135.

Rosenfeld, J.K., 1979. Amino acid diagenesis and adsorption in nearshore anoxic sediments. Limnology and Oceanography 24, 1014–1021.

Rudzinski, W., Everett, D.H., 1992. Adsorption of Gases on Heterogeneous Surfaces. Academic Press Inc., San Diego, CA.

Schwarzenbach, R., Gschwend, P.M., Imboden, D.M., 1993. Environmental Organic Chemistry. John Wiley & Sons, Inc., New York.

Sips, R., 1948. Journal of Chemical Physics 16, 490–495.

Smith, J.V., Arnold Jr., F.P., Parsons, I., Lee, M.R., 1999. Biochemical evolution III: polymerization on organophilic silica-rich surfaces, crystal-chemical modeling, formation of first cells, and geological clues. Proceedings of the National Academy of Science 96, 3479–3485.

Sposito, G., 1984. The Surface Chemistry of Soils. Oxford University Press, New York.

Su, T.J., Lu, J.R., Thomas, R.K., Cui, Z.F., Penfold, J., 1998. The conformational structure of bovine serum albumin layers

adsorbed at the silica-water interface. Journal of Physical Chemistry B 102, 8100–8108.

Sun, H., 1998. COMPASS: An *ab initio* force-field optimized for condensed-phase applications—overview with details on alkane and benzene compounds. Journal of Physical Chemistry 102, 7338.

Takahashi, H., Li, B., Sasaki, T., Miyazaki, C., Kajino, T., Inagaki, S., 2001. Immobilized enzymes in ordered mesoporous silica materials and improvement of their stability and catalytic activity in an organic solvent. Microporous and Mesoporous Materials 44-45, 755–762.

Temuujin, J., Okada, K., MacKenzie, K.J.D., 2003. Preparation of porous silica from vermiculite by selective leaching. Applied Clay Science 22, 187–195.

Theng, B.K.G., 1974. Chemistry of Clay-Organic Reactions. Wiley, New York.

Titley, J.G., Glegg, G.A., Glasson, D.R., Millward, G.E., 1987. Surface areas and porosities of particulate matter in turbid estuaries. Continental Shelf Research 7, 1363–1366.

Torn, M.S., Trumbore, S.E., Chadwick, O.A., Vitousek, P.M., Hendricks, D.M., 1997. Mineral control of soil organic carbon storage and turnover. Nature 389, 170–173.

Umpleby, R.J., Baxter, S.B., Chen, Y., Shah, R.N., Shimizu, K.D., 2001. Characterization of molecularly imprinted polymers with the Langmuir-Freundlich isotherm. Analytical Chemistry 73, 4584–4591.

Vermohlen, K., Lewandowski, H., Narres, H.-D., Koglin, E., 2000. Adsorption of polyacrylic acid on aluminum oxide: DRIFT spectroscopy and *ab initio* calculations. Colloids and Surfaces A 170, 181–189.

Vianna-Soares, C.D., Kim, C.J., Borenstein, M.R., 2002. Use of hydrophilic hydroxypropyl methacrylate/ethylene glycol methacrylate packing material in size-exclusion chromatography. Journal of AOAC International 85, 1308–1315.

Vrieling, E.G., Beelen, T.P.M., van Santen, R.A., Gieskes, W.W.C., 1999. Diatom silicon biomineralization as an inspirational source of new approaches to silica production. Journal of Biotechnology 70, 39–51.

Wang, X.-C., Lee, C., 1993. Adsorption and desorption of aliphatic amines, amino acids and acetate by clay minerals and marine sediments. Marine Chemistry 44, 1–23.

Wang, Y., Bryan, C., Xu, H., Pohl, P., Yang, Y., Brinker, J., 2002. Interface chemistry of nanostructured materials: Ion adsorption on mesoporous alumina. Journal of Colloid and Interface Science 254, 23–30.

Webb, P.A., Orr, C., 1997. Analytical Methods in Fine Particle Technology. Micromeretics Instrument Corp., Norcross, GA.

Werth, C.J., Reinhard, M., 1997. Effects of temperature on trichloroethylene desoprtion from silica gel and natural sediments. 1. Isotherms. Environmental Science and Technology 31, 689–696.

Xia, G., Ball, W.P., 1999. Adsorption-partitioning uptake of nine low-polarity organic chemicals on a natural sorbent. Environmental Science and Technology 33, 262–269.

Xing, B., Pignatello, J.J., 1997. Dual-mode sorption of low-polarity compounds in glassy poly(vinyl chloride) and soil organic matter. Environmental Science and Technology 31, 792–799.

Xing, B., Pignatello, J.J., Gigliotti, B., 1996. Competitive sorption between atrazine and other organic compounds in soils and model sorbents. Environmental Science and Technology 30, 2432–2440.

Yiu, H.H.P., Wright, P.A., Botting, N.P., 2001. Enzyme immobilization using siliceous mesoporous molecular sieves. Microporous and Mesoporous Materials 44- 45, 763–768.

Yoon, J.-Y., Kim, J.-H., Kim, W.-S., 1999. The relationship of interaction forces in the protein adsorption onto polymeric microspheres. Colloids and Surfaces A 153, 413–419.

Yoon, J.-Y., Park, H.-Y., Kim, J.-H., Kim, W.-S., 1996. Adsorption of BSA on highly carboxylated microspheres—quantitative effects on surface functional groups and interaction forces. Journal of Colloid and Interface Science 177, 613–620.

Zang, X., Nguyen, R.T., Harvey, H.R., Knicker, H., Hatcher, P.G., 2001. Preservation of proteinaceous material during the degradation of the green algae *Botryococcus braunii*: A solid-state 2D ^{15}N ^{13}C NMR spectroscopy study. Geochimica et Cosmochimica Acta 65, 3299–3305.

Zang, X., van Heemst, J.D.H., Dria, K.J., Hatcher, P.G., 1997. Encapsulation of protein in humic acid from a histosol as an explanation for the occurrence of organic nitrogen in soil and sediment. Organic Geochemistry 31, 679–695.

Zhang, H., Bloom, P.R., Nater, E.A., 1993. Change in surface area and dissolution rates during hornblende dissolution at pH 4.0. Geochimica et Cosmochimica Acta 57, 1681–1689.

Zibilske, L.M., 1994. Carbon mineralization. In: Weaver, R. (Ed.), Methods of Soil Analysis, Part 2. Microbiological and Biochemical Properties. 5 Soil Science Society of America Book Series. Soil Science Society of America, Inc., Madison, WI, pp. 835–863.

Zimmerman, A.R., Canuel, E.A., 2001. Bulk organic matter and lipid biomarker composition of Chesapeake Bay surficial sediments as indicators of environmental processes. Estuarine, Coastal and Shelf Science 53, 319–341.